

# Submission ID 56743aa6-4c8b-4718-b4c7-b1d969366ec3

 MRE Press

---

## Document Details

**Submission ID**

trn:oid:::9177:73480831

**Submission Date**

Dec 9, 2024, 3:34 PM GMT+8

**Download Date**

Dec 9, 2024, 3:36 PM GMT+8

**File Name**

24328425023715572924\_Submission ID 56743aa6-4c8b-4718-b4c7-b1d969366ec3.docx

**File Size**

108.7 KB

15 Pages





4,389 Words

26,057 Characters




# 13% Overall Similarity

The combined total of all matches, including overlapping sources, for each database.

## Match Groups

-  **61 Not Cited or Quoted 13%**  
Matches with neither in-text citation nor quotation marks
-  **3 Missing Quotations 0%**  
Matches that are still very similar to source material
-  **0 Missing Citation 0%**  
Matches that have quotation marks, but no in-text citation
-  **0 Cited and Quoted 0%**  
Matches with in-text citation present, but no quotation marks

## Top Sources

- 11%  Internet sources
- 8%  Publications
- 0%  Submitted works (Student Papers)

## Integrity Flags

### 0 Integrity Flags for Review

No suspicious text manipulations found.




Our system's algorithms look deeply at a document for any inconsistencies that would set it apart from a normal submission. If we notice something strange, we flag it for you to review.

A Flag is not necessarily an indicator of a problem. However, we'd recommend you focus your attention there for further review.

## Match Groups

- **61 Not Cited or Quoted 13%**  
Matches with neither in-text citation nor quotation marks
- **3 Missing Quotations 0%**  
Matches that are still very similar to source material
- **0 Missing Citation 0%**  
Matches that have quotation marks, but no in-text citation
- **0 Cited and Quoted 0%**  
Matches with in-text citation present, but no quotation marks

## Top Sources

- 11%  Internet sources
- 8%  Publications
- 0%  Submitted works (Student Papers)

## Top Sources

The sources with the highest number of matches within the submission. Overlapping sources will not be displayed.

1	Internet		
		www.ncbi.nlm.nih.gov	2%
2	Internet		
		www.frontiersin.org	1%
3	Publication		
		Zhi-Hui Guan, Di Yang, Yi Wang, Jia-Bin Ma, Guo-Nian Wang. "Ectodysplasin-A2 rec...	1%
4	Publication		
		Zeyu Xing, Mingyang Du, Yanhua Zhen, Jie Chen, Dongdong Li, Ruyin Liu, Jiahe Zh...	1%
5	Publication		
		Yang Wang, Chun Wang, Yue Zhang, Guan Wang, Haitao Yang. "Pre-administratio...	1%
6	Internet		
		www.spandidos-publications.com	1%
7	Publication		
		Yu Jin, Lei Zhao, Shuhao Wang, Xianglan Zhang, Jishu Quan, Zhenhua Lin, Junjie Pi...	0%
8	Internet		
		assets.researchsquare.com	0%
9	Publication		
		Runxiao Lv, Lili Du, Lunhao Bai. "RNF125, transcriptionally regulated by NFATC2, ...	0%
10	Internet		
		www.nature.com	0%

11	Internet	www.aging-us.com	0%
12	Internet	www.researchsquare.com	0%
13	Internet	cyberleninka.org	0%
14	Internet	link.springer.com	0%
15	Internet	onlinelibrary.wiley.com	0%
16	Internet	journals.plos.org	0%
17	Publication	Fengjiao Huo, Qing Liu, Shuyao Lv, Yue Liu et al. "Disruption of the Circadian Rhyt..."	0%
18	Internet	clincalepigeneticsjournal.biomedcentral.com	0%
19	Internet	www.jcancer.org	0%
20	Internet	www.jstage.jst.go.jp	0%
21	Internet	www.oncotarget.com	0%
22	Internet	aacrjournals.org	0%
23	Internet	www.biorxiv.org	0%
24	Publication	Yi-Lian Wang, Dong Cao, Qiong Ding, Wubin Yu, Ming Gao. "Long noncoding RNA ..."	0%

25	Internet	portlandpress.com	0%
26	Internet	translational-medicine.biomedcentral.com	0%
27	Publication	Fang Wang, Yalong Dang, Jing Wang, Ting Zhou, Yu Zhu. "Gypenosides attenuate ...	0%
28	Publication	Lin Xin, Li Liu, Chuan Liu, Li-Qiang Zhou, Qi Zhou, Yi-Wu Yuan, Shi-Hao Li, Hou-Tin...	0%
29	Publication	Yanhong Gu, Xiao Zhang, Shurui Cao, Chenchen Zhou, Wen Jiang, Xiaheng Deng, ...	0%
30	Publication	Yu Bai, Qiang Du, Le Zhang, Ling Li, Lei Tang, Wei Zhang, Runyu Du, Ping Li, Ling ...	0%
31	Publication	Chen Zhang, Yue Sun, Yingying Guo, Jingjing Xu, Haiyan Zhao. "JMJD1C promotes ...	0%
32	Publication	Haiyun Xie, Jiangfeng Li, Yufan Ying, Huaqing Yan et al. " METTL3/YTHDF2 m A axi...	0%
33	Publication	Zhi-Hui GUAN, Di YANG, Yi WANG, Jia-Bin MA, Guo-Nian WANG. "EDA2R knockdow...	0%

## 1 **Abstract**

### 2 **Background**

7 RING finger protein 112 (RNF112) exerts a key role in human tumors. However, its  
4 biological function in colorectal cancer (CRC) has not been discussed. We aimed to  
7 explore the function and molecular mechanism of RNF112 in CRC.

### 6 **Results**

7 In this study, RNF112 expression was notably decreased in CRC tissues and cells.  
8 Clinical analysis revealed a significant association between low RNF112 expression  
9 and tumor size, N classification and TNM stage. *In vitro* experiments demonstrated that  
10 overexpression of RNF112 repressed cell viability, promoted cell cycle arrest and  
11 apoptosis, while knocking down RNF112 had the opposite function. The tumor  
12 formation results in nude mice supported that RNF112 overexpression exerted anti-  
13 tumor effects by inhibiting cell growth and promoting cell apoptosis. Mechanistically,  
14 Krüppel-like factor 4 (KLF4) acted as an upstream regulator of RNF112 by mediating  
15 its transcription. Furthermore, we explored the downstream mechanism of RNF112 and  
16 discovered that it promoted ubiquitination and degradation of oncoprotein N-alpha-  
17 acetyltransferase 40 (NAA40) through ubiquitin ligase activity. In addition,  
18 overexpression of NAA40 eliminated the effect of RNF112 overexpression on CRC  
19 tumorigenesis.

### 20 **Conclusions**

21 In summary, our findings confirm that RNF112, whose transcription is regulated by  
22 KLF4, inhibits CRC growth through promoting ubiquitin-dependent degradation of  
23 NAA40. We have unraveled the mechanism of KLF4-RNF112-NAA40 axis in CRC,  
24 which shed light on the therapeutic strategies for this disease.

25 **Keywords:** colorectal cancer; RNF112; KLF4; NAA40; ubiquitination

### 24 **Introduction**

27 Colorectal cancer (CRC) is one of the most common cancers (Li et al. 2022). Recently,  
28 the incidence of CRC patients has continued to increase (Biller and Schrag 2021). Many  
29 CRC patients will develop metastasis at diagnosis or follow-up (Vayrynen et al. 2020).

30 Although chemotherapy is generally recommended, only a few targeted therapies are  
31 suitable for cases with specific mutational signatures (Xu et al. 2021). Therefore, the  
32 development of novel molecular targets against CRC is imminent.

33 RING finger protein 112 (RNF112) has been identified as an E3 ubiquitin ligase (Pao  
34 et al. 2011). RNF112 exerted a vital role in neuronal differentiation (Tsou et al. 2017;  
35 Wang et al. 2015). RNF112 showed a protective effect on intracerebral hemorrhage  
36 through suppressing the TLR-4/NF- $\kappa$ B pathway (Zhang and Zhang 2018). Notably,  
37 RNF112 has been demonstrated to participate in cancer progression. Knockdown of  
38 RNF112 reduced expression of the negative cell cycle regulators p35 and p27, leading  
39 to cell cycle reprogramming in embryonal carcinoma (Pao et al. 2011). RNF112 blocked  
40 the malignant behavior of glioma cells via the p53-mediated cell cycle signaling  
41 pathway (Lee et al. 2017). RNF112 impeded gastric cancer process by promoting  
42 ubiquitination of FOXM1 (Zhang et al. 2023). RNF112 may be a promising prognostic  
43 biomarker for CRC (Yang et al. 2024). Strikingly, data from mRNA sequencing and  
44 GEO databases presented that RNF112 expression was remarkably downregulated in  
45 CRC tissues. However, the biological role of RNF112 in CRC has never been discussed.

46 Krüppel-like factor 4 (KLF4), a member of the evolutionarily conserved zinc finger  
47 transcription factor family, regulates many physiological processes (He et al. 2023).  
48 Accumulating evidence suggested that KLF4 was a potential tumor suppressor in CRC.  
49 For instance, KLF4 inhibited CRC cell proliferation through transcriptional activation  
50 of NDRG2 (Ma et al. 2017). KLF4 also enhanced the sensitivity of HCT-15 cells to  
51 cisplatin (Yadav et al. 2019). Notably, data from mRNA sequencing and GEO databases  
52 revealed that KLF4 expression was obviously lower in CRC tissues than in controls. In  
53 addition, JASPAR database predicted the possible binding sites of KLF4 in the RNF112  
54 promoter. However, whether RNF112 is transcriptionally modulated by KLF4 in CRC  
55 remains to be confirmed.

56 N-alpha-acetyltransferase 40 (NAA40) belongs to NAT family (Hole et al. 2011).  
57 Increasing studies indicated that NAA40 played a carcinogenic role in CRC. NAA40-  
58 mediated metabolic recombination promoted CRC cell resistance to anti-metabolic  
59 drug chemotherapy (Demetriadou et al. 2022). NAA40 facilitated CRC progression by

60 controlling PRMT5 expression (Demetriadou et al. 2019). Depletion of NAA40  
61 induced cell apoptosis in CRC (Pavlou and Kirmizis 2016). Of note, IP-LC/MS and  
62 Label-Free assays suggested that NAA40 may be a downstream target protein of  
63 RNF112, but whether NAA40 affects the function of RNF112 in CRC needs further  
64 confirmation.

65 Here, we want to explore the capabilities of RNF112 in CRC and its potential  
66 mechanisms.

## 67 **Materials and methods**

### 68 **mRNA sequencing**

11 69 Clinical study was approved by the Medical Ethics Committee of Shengjing Hospital  
70 of China Medical University and conducted based on the Declaration of Helsinki. All  
71 subjects provided written informed consent. mRNA sequencing was conducted using  
72 22 CRC tissue samples and 18 adjacent tissue samples by Wuhan Yingzi Gene  
73 Technology Co., Ltd. Sample information was shown in supplementary Table 1. Data  
74 analysis of mRNA sequencing was as follows: the original sequencing data was  
75 obtained through data quality control. Clean data was compared to the reference  
76 genome of the corresponding species. Based on the comparison results, the library  
77 quality was evaluated, and the sample library data qualified for quality control was  
78 analyzed.

### 79 **Bioinformatics analysis**

2 80 GSE200427 chip (<https://www.ncbi.nlm.nih.gov/geo/query/acc.cgi?acc=GSE200427>)  
18 81 containing 2 normal samples and 2 CRC samples and GSE196006 chip  
82 (<https://www.ncbi.nlm.nih.gov/geo/query/acc.cgi?acc=GSE196006>) containing 21  
2 83 normal samples and 21 CRC samples were download from NCBI. Differentially  
84 expressed genes (DEGs,  $|\log_2FC| > 1$  and  $p < 0.01$ ) were identified. GO and KEGG  
85 enrichment analysis was then carried out. In addition, list of genes related to E3 ligase  
86 was retrieved from GeneCards (<https://www.genecards.org/>) database using “E3  
87 ubiquitin ligases” as a keyword. Ubiquitin ligase coding and related genes in gene class  
10 88 were obtained from UALCAN database ([3](https://ualcan.path.uab.edu/cgi-bin/Kinase-</a></p></div><div data-bbox=)



89 summary2.pl).

## 90 **Clinical samples detection**

91 Twenty-nine pairs of fresh primary CRC and adjacent tissues, as well as 92 paraffin-  
92 embedded CRC tissues were collected. RNF112 levels were evaluated by  
93 immunohistochemistry using a scoring method (Zheng et al. 2022).

## 94 **Immunohistochemistry**

15 95 Sections were dewaxed and rehydrated. Afterwards, endogenous peroxidase was  
96 blocked with 3% H<sub>2</sub>O<sub>2</sub> for 15 min. RNF112 (1:100, PA5-118985, Thermo Fisher, USA)  
31 97 or Ki67 (1:100, AF0198, Affinity, Changzhou, China) antibodies were incubated  
12 98 overnight at 4°C, followed by secondary antibody (1:200, D110058, Sangon, Shanghai,  
99 China) at 37°C for 0.5 h. DAB was used to develop, and staining was acquired with a  
100 microscope.

## 101 **Cell culture**

1 102 GP2D and SW1116 cells were obtained from iCell (Shanghai, China). DLD1 and  
1 103 SW620 and NCM460 cells were obtained from Cellverse (Shanghai, China). DLD1,  
1 104 GP2D and NCM460 cells were cultured in 1640 (Solarbio, Beijing, China). SW1116  
13 105 and SW620 cells were cultured in L-15 (Procell, Wuhan, China). Cells were placed at  
106 37°C and 5% CO<sub>2</sub>.

## 107 **Knockdown and overexpression**

108 siRNAs targeting RNF112 were synthesized from JinTuoSi (Wuhan, China). shRNAs  
109 targeting RNF112 were cloned to pRNAH1.1 vector. In addition, KLF4 CDS, RNF112  
110 CDS or NAA40 CDS were cloned to pcDNA3.1 vector. Cells were transfected using  
111 Liposome 3000 (Invitrogen, USA).

112 siRNAs targeting RNF112 were shown:

113 RNF112<sub>siRNA-1</sub>, CCUGAGUGCCGGAAGAUAU;

114 RNF112<sub>siRNA-2</sub>, CCUUCCUCCUCAACCAUUU;

115 RNF112<sub>siRNA-3</sub>, GGUGAUGGGCAAGCAUUUAU;

116 RNF112<sub>siRNA-4</sub>, AGAGAUUGUCUGGCAGAUUAU;

117 RNF112<sub>siRNA-5</sub>, CACCCAGAAAGAUGCCAUU.

118 shRNAs targeting RNF112 were shown:

119 RNF112<sub>shRNA-1</sub>, GGAAGATATGCAAGCAGAATTCAAGAGATTCTGCTTGC  
120 ATATCTTCCTTTTT;

121 RNF112<sub>shRNA-2</sub>, GGAAGTCCTTCCTCCTCAATTCAAGAGATTGAGGAGGA  
122 AGGACTTCCTTTTT.

### 123 Cell viability analysis

8 124 Cells ( $5 \times 10^3$ / well) were seeded in 96-well plates. Next, after 48 h and 72 h, CCK8  
33 125 reagent (KeyGEN, Nanjing, China) was added. Finally, OD 450 was tested on a  
126 microplate reader (Biotek, USA).

### 127 Flow cytometry detection

3 128 For cell cycle, cells were treated with 500  $\mu$ l PI/RNase A (KeyGEN) and incubated for  
129 30 min. For apoptosis, cells were treated with 5  $\mu$ l AnnexinV-FITC and 5  $\mu$ l PI and  
3 130 incubated for 10 min. Finally, data was measured by a NovoCyte flow cytometer.

### 131 Caspase 3 and Caspase 9 activity

132 Caspase-3 (C1116, Beyotime, Shanghai, China) and Caspase-9 activity (C1158,  
133 Beyotime) was tested by the respective kits.

### 134 Xenotransplantation

4 135 Animal studies were approved by Medical Ethics Committee of Shengjing Hospital of  
8 136 China Medical University and in lines with the National Research Council's Guide for  
21 137 the Care and Use of Laboratory Animals. After 1 week of adaptive feeding, BALB/c  
138 nude mice (4-week-old) were divided into 5 groups (vector, RNF112<sub>OE</sub>, NC, RNF112  
139<sub>shRNA-1</sub> and RNF112<sub>shRNA-2</sub>). SW620 or DLD1 cells ( $2 \times 10^6$ ) were injected  
28 140 subcutaneously. Tumor size was measured every 5 days. After 4 weeks, mice were  
141 killed and tumor tissues were collected.

### 142 TUNEL staining

14 143 After deparaffinized and hydrated, sections were treated with 0.1% Triton X-100 (50  
3 144  $\mu$ l, Beyotime) for 8 min and 50  $\mu$ l TUNEL solution for 1 h. Afterwards, sections were  
145 stained with DAPI for 5 min, and staining was acquired under a microscope.

### 146 Prediction of binding of KLF4 to RNF112 promoter

20 147 RNF112 promoter was retrieved through the UCSC Genome Browser Gateway  
148 database ([https://genome-asia.ucsc.edu/cgi-bin/hgGateway?hgid=730609074\\_3yH3](https://genome-asia.ucsc.edu/cgi-bin/hgGateway?hgid=730609074_3yH3))

149 QyIyhAexYB3spswXoIohivRN), and the promoter sequence was pasted into the  
150 JASPAR database (<https://jaspar.elixir.no/>). Binding sites of KLF4 on the RNF112  
151 promoter were predicted.

### 152 **Luciferase reporter assay**

153 Luciferase reporter vector containing the promoter sequence of RNF112 was  
154 constructed and transferred into SW620 cells with KLF4 overexpression plasmid. pRL-  
155 TK was a control plasmid. Finally, luciferase activity was measured 48 h later.

### 156 **Chromatin-immunoprecipitation (Ch-IP) assay**

9 157 Cells were incubated with 1% formaldehyde for 1 h and 10X Glycine Solution. Cells  
9 158 precipitates were then resuspended in SDS lysis. After ultrasonic treatment, 1.8 ml Ch-  
159 IP dilution buffer was added to 0.2 ml supernatant. 20  $\mu$ l supernatant was used as input,  
17 160 and the remain supernatant was added to 70  $\mu$ l Protein A+G Agarose/Salmon Sperm  
161 DNA. After centrifugation, supernatant was added with 1  $\mu$ g KLF4 antibody (11880-1-  
22 162 AP, Proteintech) or IgG. Then the mixture was treated with 60  $\mu$ l Protein A+G  
163 Agarose/Salmon Sperm DNA. Afterwards, DNA-protein complex was added with 5 M  
164 NaCl, and the purified DNA was used for PCR assay. PCR primers were as follows:

165 Ch-IP-1

16 166 F: 5'-CCTGCCTTGACAACCTTT-3'

167 R: 5'-GATGGGACAATCAGTCTTCAC-3'

168 Ch-IP-2

169 F: 5'-GGTAATGGTGGCTCCTC-3'

170 R: 5'-CCTTCTCATCCCTCCTG-3'

### 171 **Co-immunoprecipitation (Co-IP)**

172 Cells were lysed and proteins were isolated. The antibody was immobilized, and IP was  
173 performed. In brief, IP lysate (200  $\mu$ l) was added to the resin that solidified the antibody.  
174 After elution, the obtained samples were used for western blot.

### 175 **Ubiquitination assay**

9 176 For ubiquitination analysis, cells were treated with 10  $\mu$ M MG132 for 8 h. Western blot  
177 was used to detect ubiquitination levels.

### 178 **IP-LC/MS and Label-Free assays**

179 RNF112 overexpression vector (with Flag tag) and its control vector (with Flag tag)  
180 were constructed and transfected into SW620 cells, respectively. After 48 h, IP-LC/MS  
181 analysis was performed on the vector-Flag and RNF112-Flag from anti-Flag by  
182 Novogene (Beijing, China). According to the files detected, the corresponding database  
183 was searched for protein identification. At the same time, mass tolerance distribution  
184 of polypeptide, protein and parent ion was analyzed to evaluate the quality of mass  
185 spectrometry data.

186 RNF112 overexpression vector or its control vector were transfected into SW620  
187 cells, respectively. After 48 h, cells were employed for Label-Free. Label-Free was  
188 conducted by Qinglian Baiao Technology Co., Ltd. (Beijing, China) in accordance with  
189 a standard experimental procedure. Differentially expressed proteins ( $|\log_2FC| > 1$  and  
190  $p < 0.05$ ) were identified. Proteins were then subjected to GO and KEGG enrichment  
191 analysis.

## 192 Immunofluorescence double staining

193 After blocking with 1% BSA, sections were incubated with Flag (1: 100, 66008-4-Ig,  
194 Proteintech) and NAA40 (1: 100, 16698-1-AP, Proteintech) antibodies at 4°C overnight,  
195 followed by respective secondary antibodies (1: 200, #4408, CST, USA or 1: 200,  
196 #4413, CST) for 1 h. Finally, after treating with DAPI, sections were pictured with a  
197 microscope.

## 198 Real-time PCR

199 Total RNA was extracted with TRIpure. Next, RNA was transcribed into cDNA by All-  
200 in-One First-Strand SuperMix (Magen, Guangzhou, China). Afterwards, real-time PCR  
201 was conducted with the SYBR Green kit (Solarbio). Relative mRNA levels were  
202 calculated with a  $2^{-\Delta\Delta C_t}$  method. Primers were shown as follows:

203 RNF112, F: 5'-GGACAGACGCCTACTCACG-3';  
204 RNF112, R: 5'-CTGCCTCACATACTCCTCGA-3';  
205 KLF4, F: 5'-CCAGAGGAGCCCAAGCCAAAG-3';  
206 KLF4, R: 5'-TCCACAGCCGTCCCAGTCA-3';  
207  $\beta$ -actin F: 5'-GGCACCCAGCACAATGAA-3';  
208  $\beta$ -actin R: 5'-TAGAAGCATTGCGGTGG-3'.

## 209 **Western blot**

210 Total protein was extracted and quantified by BCA assay kit (Beyotime). 20 µg protein  
211 was loaded into each well of a 10% SDS-PAGE gel and transferred to PVDF  
212 membranes (Abcam, UK). Next, the blots were incubated with RNF112 (1:1000, PA5-  
213 118985, Thermo Fisher), Cyclin E1 (1:1000, 11554-1-AP, Proteintech), CyclinD1  
214 (1:5000, 26939-1-AP, Proteintech) and NAA40 (1:500, 16698-1-AP, Proteintech)  
215 antibodies overnight at 4°C. Thereafter, the blots were incubated with HRP-labeled goat  
216 anti-rabbit IgG (1:5000, A0208, Beyotime) or goat anti-mouse IgG (1:5000, A0216,  
217 Beyotime) at 37°C for 45 min. Finally, the blots were treated with ECL reagent, and  
218 data were then analyzed by Gel-Pro-Analyzer software.

## 219 **Statistical analysis**

220 In this study, data are expressed as mean±SD. Data between two groups were compared  
221 by student's t-test. Data of multiple groups were compared by one-way or two-way  
222 ANOVA. Correlation between RNF112 expression and clinicopathological features was  
223 analyzed by Chi-square test. Additionally, correlation between RNF112 mRNA and  
224 KLF4 mRNA was evaluated by Pearson.  $p < 0.05$  was considered statistically significant.

## 225 **Results**

### 226 **RNF112 may be involved in CRC tumorigenesis**

227 To screen potential molecular targets of CRC, we performed mRNA sequencing  
228 using CRC tissue samples and adjacent tissue samples. In addition, we downloaded  
229 GSE200427 and GSE196006 chips from NCBI and then carried out bioinformatic  
230 analysis of the DEGs in these three databases. Firstly, the ring heat map and volcano  
231 map showed the expression of genes in the three datasets. There were 1,534 upregulated  
232 genes and 1,504 downregulated genes in mRNA sequencing results (Figure 1A). In  
233 GSE200427 dataset, there were 801 upregulated genes and 1128 downregulated genes  
234 (Figure 1A). In addition, in GSE196006 dataset, there were 1,634 upregulated genes  
235 and 1,537 downregulated genes (Figure 1A). GO and KEGG analysis were conducted.  
236 BP results presented that DEGs were enriched in mitotic cell cycle phase transition,  
237 DNA-templated DNA replication and regulation of ubiquitin protein ligase activity

238 (Figure 1B). CC data indicated that DEGs were enriched in cyclin-dependent protein  
239 kinase holoenzyme complex and DNA replication preinitiation complex (Figure 1B).  
240 MF results suggested that DEGs were enriched in growth factor activity and chemokine  
241 receptor binding (Figure 1B). Moreover, KEGG enrichment analysis showed that DEGs  
242 participated in cytokine-cytokine receptor interaction, PI3K-Akt signaling pathway and  
243 cell cycle (Figure 1B). Upset chart was used to show the number of crossed genes in  
244 the three datasets. We found that 24 DEGs had intersections in the three databases  
245 (Figure 1C). We further screened the target factors based on the results of three  
246 databases. Firstly, we intersected the DEGs of the three datasets to obtain 766 common  
247 DEGs. Next, the 766 common DEGs were intersected with genes related to E3  
248 Ubiquitin ligase in GeneCards and ubiquitin ligase coding and related genes in  
249 UALACN database to obtain 6 shared DEGs, including RNF112, UHRF1, ENC1,  
250 CCNF, RNF183 and NEDD4L (Figure 1D). By investigating the function of these 6  
251 DEGs, we found that only the function of RNF112 in CRC was unknown, so RNF112  
252 was selected as a target for subsequent analysis.

### 253 **RNF112 expression was obviously decreased in CRC tissues and cells**

254 Firstly, we set out to explore the expression of RNF112 in CRC tissues. Data from  
255 transcriptome sequencing and GSE200427 and GSE196006 chips showed that RNF112  
256 was obviously decreased in CRC tissues (Figure 1A). Results from the UALCAN  
257 database also indicated that RNF112 levels were markedly reduced in colon cancer  
258 tissues in comparison with the controls (Figure 2A). In addition, we collected 29 pairs  
259 of adjacent and tumor tissues from CRC patients. Figure 2B-C displayed that RNF112  
260 expression was overtly decreased in tumor tissues. Immunohistochemistry assay  
261 presented that RNF112 levels were increased in adjacent tissues, but gradually  
262 decreased in TNM stage (Figure 2D). To explore the clinicopathological significance of  
263 RNF112 in CRC, the correlation between RNF112 expression and the pathologic  
264 materials was explored. The analysis suggested that RNF112 low expression was  
265 correlated with tumor size, N classification and TNM stage (Table 1).

266 Furthermore, the abundance of RNF112 was remarkably decreased in the CRC cells  
267 including GP2D, SW1116, DLD1 and SW620, compared to NCM460 (Figure 2E). In

268 addition, we found that RNF112 was moderately expressed in SW620 and DLD1 cells.  
269 Therefore, siRNAs targeting RNF112 and its control NC, as well as RNF112  
270 overexpression plasmid and its vector plasmid were transfected into SW620 and DLD1  
271 cells, respective. After transfection for 48 h, the knockdown and overexpression  
272 efficiency of RNF112 was verified. These findings indicated that RNF112 was  
273 successfully knocked down or overexpressed in CRC cells (Figure S1A-B).

#### 274 **Overexpression of RNF112 suppressed the proliferation of CRC cells**

275 We elucidated the precise role of RNF112 in CRC tumor biology. Functional  
276 experiments were carried out after RNF112 overexpression or knockdown.  
277 Phenotypically, overexpression of RNF112 repressed cell viability and triggered cell  
278 cycle arrest in G1 phase in CRC cells, however, RNF112 knockdown exhibited the  
279 opposite effect (Figure 3A-B). Notably, RNF112 overexpression also inhibited the  
280 expression of cyclin E1 and cyclinD1, while RNF112 knockdown elevated their protein  
281 levels (Figure 3C). Taken together, we elucidated that RNF112 suppressed CRC cell  
282 viability and cell cycle progression.

#### 283 **Overexpression of RNF112 promoted the apoptosis of CRC cells**

284 Furthermore, we ascertained the function of RNF112 on apoptosis. Firstly, our results  
285 indicated that overexpression of RNF112 distinctly enhanced apoptosis (Figure 4A).  
286 We also assessed the impact of RNF112 on the levels of proapoptotic markers and  
287 discovered that overexpression of RNF112 upregulated caspase 3 and caspase 9 activity  
288 (Figure 4B). Therefore, these data uncovered that RNF112 overexpression promoted  
289 CRC cell apoptosis.

#### 290 **Overexpression of RNF112 repressed the growth of CRC cells *in vivo***

291 We also determined whether RNF112 is involved in the tumorigenesis of CRC *in vivo*.  
292 RNF112 overexpression significantly retarded xenograft tumor growth, as expected,  
293 RNF112 knockdown exhibited the opposite effect (Figure 5A). In addition, we  
294 investigated the role of RNF112 in the expression of tumor growth marker Ki67 (Menon  
295 et al. 2019). Immunohistochemistry results illustrated that RNF112 overexpression  
296 decreased Ki67 expression, while RNF112 knockdown increased its expression (Figure  
297 5B). The knockdown and overexpression efficiency of RNF112 was also tested by

298 immunohistochemistry, indicating that RNF112 was successfully overexpressed or  
299 knocked down (Figure 5B). TUNEL staining was used to assess the impact of RNF112  
300 on apoptosis, and the results demonstrated that RNF112 overexpression increased  
301 TUNEL-positive cells, supporting its pro-apoptotic effect (Figure 5C). Collectively, our  
302 findings confirmed that overexpression of RNF112 repressed the growth of CRC cells  
303 *in vivo*.

#### 304 **KLF4 promoted the transcriptional regulation of RNF112**

305 Here, we set out to identify the transcriptional mechanism of RNF112 in CRC. Firstly,  
306 the transcription factors predicted by TFtarget database to bind to the RNF112 promoter  
307 region were intersected with 766 common DEGs to obtained 2 DEGs, including KLF4  
308 and TCF21 (Figure 6A). Next, real-time PCR assay indicated that KLF4 levels were  
309 notably downregulated in CRC tissues compared to adjacent tissues (Figure 6B). The  
310 correlation of KLF4 mRNA and RNF112 mRNA in mRNA sequencing and CRC  
311 clinical samples was then explored. The analysis indicated that their expression was  
312 positively correlated (Figure 6C). Furthermore, KLF4 overexpression significantly  
313 upregulated KLF4 and RNF112 mRNA levels in SW620 cells (Figure 6D). JASPAR  
314 database analysis identified the binding sites for KLF4 in the RNF112 promoter,  
315 suggesting that KLF4 may regulate the transcription of RNF112. To test this possibility,  
316 we conducted a luciferase reporter assay to interrogate the regulation mode of KLF4 on  
317 RNF112. As reflected, exogenous KLF4 stimulated a significant increase in luciferase  
318 activity at -1801~-+15bp and -2000~-+15bp of the promoter region of RNF112 in CRC  
319 cells (Figure 6E). Ch-IP experiments suggested that two motifs of KLF4 bound to the  
320 promoter region of RNF112 (Figure 6F). Therefore, our data revealed that KLF4 was a  
321 transcription factor involved in regulating RNF112 expression.

#### 322 **NAA40 was a downstream protein of RNF112**

323 To probe the mechanism downstream of RNF112, IP-LC/MS and Label-Free were  
324 conducted. Firstly, 48 h after transfection, the levels of RNF112-Flag in Co-IP  
325 precipitation were determined by immunoblotting (Figure 7A). Co-IP precipitates were  
326 then subjected to gel electrophoresis and stained with Coomassie Brilliant Blue (Figure  
327 7B). IP-LC/MS and Label-Free assays were performed. Label-Free PCA analysis



328 showed that vector samples and RNF112 overexpression samples were clustered,  
329 respectively (Figure 7C). We found that RNF112 overexpression resulted in significant  
330 downregulation of 26 proteins and upregulation of 59 proteins (Figure 7D). GO  
331 enrichment results showed that these proteins were related to regulation of mitotic cell  
332 cycle phase transition, RNA polymerase II transcription regulator complex and DNA-  
333 binding transcription factor binding (Figure 7E). KEGG data implied that these proteins  
334 participated in cellular senescence, p53 signaling pathway and cell cycle (Figure 7F).  
335 Finally, 2265 binding proteins of RNF112 in the IP-LC/MS results were cross-analyzed  
336 with the downregulated proteins in the Label-Free results, and 5 common proteins were  
337 obtained, including CRABP2, LGALS1, NAA40, NMD3 and MMAB (Figure 7G). By  
338 inquiring the function of these 5 proteins, it was found that only NAA40 played a tumor-  
339 promoting role in CRC. But the function of the remaining 4 proteins in CRC is unknown.  
340 Thus, we speculated that NAA40 may be a downstream protein of RNF112.

#### 341 **RNF112 interacted with NAA40 and enhanced its ubiquitination degradation**

342 We further validated the regulatory mechanism of RNF112 and NAA40. Firstly,  
343 RNF112 overexpression suppressed the protein levels of NAA40, while RNF112  
344 knockdown promoted its protein levels (Figure 8A). As indicated by  
345 immunofluorescence, RNF112 and NAA40 were mainly colocalized in cytoplasm, and  
346 rarely colocalized in nucleus (Figure 8B). Co-IP assay indicated that RNF112-Flag  
347 combined with NAA40 in SW620 cells (Figure 8C). After SW620 cells were treated  
348 with MG132 for 8 h, the levels of NAA40 were detected. We noted that RNF112  
349 inhibited the expression of NAA40 via proteasome pathway (Figure 8D). As revealed  
350 in Figure 8E, overexpression of RNF112 promoted the degradation of NAA40. In  
351 addition, HEK293T cells were transfected with NAA40 and RNF112 alone or co-  
352 transfected to detect the exogenous combination of RNF112 and NAA40. Co-IP results  
353 showed a combination of the two proteins (Figure 8F). HEK293T cells were also  
354 transfected with NAA40, RNF112 and Ub. Co-IP was used to detect the ubiquitination  
355 levels. The data indicated that RNF112 promoted the ubiquitination of NAA40 (Figure  
356 8G).

357 Since RNF112 is a RING-type E3 ubiquitin ligase, we deleted its E3 ubiquitin ligase

358 activity by mutating the RING domain and named it RNF112-MUT (Figure 8H). Co-IP  
359 results showed a slight reduction in binding of RNF112-Mut and NAA40 compared to  
360 RNF112-WT and NAA40 (Figure 8I). In addition, HEK293T cells were transfected  
361 with NAA40, RNF112-WT or RNF112-Mut and Ub. It was found that RNF112-Mut  
362 reduced NAA40 ubiquitination levels compared to RNF112-WT (Figure 8J). Totally,  
363 these observations confirmed that RNF112 promoted ubiquitin-dependent degradation  
364 of NAA40.

### 365 **NAA40 overexpression diminished the impact of RNF112 overexpression on CRC** 366 **tumorigenesis**

367 To further verify whether NAA40 affects the function of RNF112 on CRC  
368 tumorigenesis, SW620 cells were transfected with RNF112 and NAA40 overexpression  
369 plasmids. As indicated by CCK8 assay, NAA40 overexpression increased cell viability  
370 that was inhibited by RNF112 overexpression (Figure 9A). Furthermore, NAA40  
371 overexpression upregulated the levels of cyclin E1 and cyclinD1, as well as  
372 downregulated caspase 3 and caspase 9 activity, further diminishing the role of RNF112  
373 overexpression in CRC (Figure 9B-C). Overall, our data certified that RNF112  
374 suppressed CRC growth by inhibiting NAA40 levels.

### 375 **Discussion**

376 As demonstrated, RNF112 reprogrammed glioma cells to a more differentiated phenotype  
377 and inhibited glioma progression through a p53-mediated cell cycle signaling  
378 pathway(Lee et al. 2017). In addition, RNF112 suppressed gastric cancer process by  
379 triggering ubiquitination of FOXM1(Zhang et al. 2023). Notably, bioinformatics  
380 analysis implied that RNF112 may be implicated in CRC. Our data further indicated  
381 that RNF112 expression was overtly decreased in CRC tissues, which was consistent  
382 with the results of transcriptome sequencing. Next, we found that the low RNF112  
383 expression was significantly correlated with tumor size, N classification and TNM stage.  
384 However, our study did not track the relationship between RNF112 levels and patient  
385 survival using clinical data. We believed that exploring the relationship between  
386 RNF112 expression and patient survival will deepen the clinical relevance of RNF112

387 in CRC prognosis, and this investigation will be conducted in future studies. Afterwards,  
388 gain or loss of function assays were conducted. Overexpression of RNF112 inhibited  
389 cell viability and cell cycle process and induced apoptosis *in vitro*, as well as reduced  
390 the tumorigenesis of CRC cells *in vivo*. As demonstrated, RNF112 knockdown showed  
391 a cancer-promoting effect. Together, our findings verified that RNF112 had an  
392 antitumor role in CRC.

393 In order to explore transcriptional regulatory mechanism of RNF112 in CRC, we  
394 analyzed its upstream transcription factors. By cross-analyzing the transcription factors  
395 bound to the RNF112 promoter region predicted by TFtarget and 766 DEGs, two genes  
396 that may regulate the transcription of RNF112 were obtained, including KLF4 and  
397 TCF21. The reason we chose KLF4 as the upstream of RNF112 is that there are more  
398 reliable reports that KLF4 plays a cancer-suppressing role in CRC (Xiu et al. 2017;  
399 Zhao et al. 2004). Downregulation of KLF4 contributed to metastasis and the epithelial-  
400 to-mesenchymal transition of CRC cells (Shao et al. 2019). KLF4 also inhibited the  
401 proliferation of CRC cells dependent on NDRG2 signaling (Ma et al. 2017). In addition,  
402 KLF4 sensitized colon cancer cell to cisplatin cytotoxicity by regulating HMGB1 and  
403 hTERT12 (Yadav et al. 2019). But the role of TCF21 in CRC is less clear. Therefore,  
404 we selected KLF4 as the transcription factor for RNF112 for follow-up studies. Notably,  
405 results of transcriptome sequencing and GEO databases illustrated that KLF4  
406 expression was largely downregulated in CRC tissues. Our further assays confirmed  
407 that KLF4 regulated RNF112 expression. Of note, JASPAR prediction analysis  
408 presented that KLF4 had potential binding sites in the RNF112 promoter. Subsequently,  
409 our data demonstrated that KLF4 bound to RNF112 promoter and promoted its  
410 transcription. Totally, our results proved that KLF4, as an upstream of RNF112,  
411 elevated its expression.

412 A previous study indicated that RNF112 mediated ubiquitination of FOXM1 and  
413 altered its stability (Zhang et al. 2023). To elucidate the downstream mechanism of  
414 RNF112, IP-LC/MS and Label-Free assays were conducted. Cross-analysis of the 2265  
415 binding proteins of RNF112 in the IP-LC/MS results with the downregulated proteins  
416 in the Label-Free results yielded 5 common proteins, including CRABP2, LGALS1,

26 417 NAA40, NMD3 and MMAB. Through the exploration of the functions of these 5  
418 proteins, only NAA40 was found to play a pro-tumor role in CRC. For instance, loss of  
419 NAA40 resulted in altered expression of key oncogenes and tumor suppressor genes  
420 that inhibit the growth of CRC cells (Demetriadou et al. 2019). Depletion of NAA40  
421 induced cell apoptosis in CRC (Pavlou and Kirmizis 2016). Therefore, NAA40 with  
422 clear function was selected as the downstream factor for study. If other factors with  
423 unknown function are selected, it is debatable whether RNF112 works through these  
424 factors. Our findings further confirmed that RNF112 interacted with NAA40 and  
425 induced its ubiquitination degradation depending on the ubiquitin ligase activity in CRC  
426 cells. Recovery assays thus demonstrated that NAA40 partially rescued the function of  
427 RNF112, not completely abolished the role of RNF112, but it also reflected that  
428 RNF112 did play a role in CRC through NAA40. These data implied that RNF112  
429 showed an anticancer effect by decreasing NAA40 expression, however, the deeper  
430 mechanisms of the two proteins still need to be further explored in the future.

## 431 **Conclusions**

432 Altgether, our findings imply that RNF112, whose transcription is regulated by KLF4,  
433 inhibits CRC growth by promoting ubiquitination and degradation of NAA40.  
434 Therefore, our study highlights the importance of the KLF4-RNF112-NAA40 signaling  
435 axis in CRC tumor biology, which may hold great promise for either diagnosis or  
436 therapy.

437